



Stemtuberolines A-G, new alkaloids from *Stemona tuberosa* and their anti-TMV activity

Zhan-Xing Hu^{a,b,1}, Qiao An^{a,b,1}, Hong-Yu Tang^{c,d}, Chun-Mao Yuan^{a,b}, Ya-Nan Li^{a,b}, Yu Zhang^{c,**}, Xiao-Jiang Hao^{a,b,c,*}

^a State Key Laboratory of Functions and Applications of Medicinal Plants, Guizhou Medical University, Guiyang 550014, PR China

^b The Key Laboratory of Chemistry for Natural Products of Guizhou Province and Chinese Academy of Sciences, Guiyang 550002, PR China

^c State Key Laboratory of Phytochemistry and Plant Resources in West China, Kunming Institute of Botany, Chinese Academy of Sciences, Kunming 650201, PR China

^d School of Chemical Science and Technology, Yunnan University, Kunming 650091, PR China

ARTICLE INFO

Keywords:

Stemona tuberosa
Tuberostemoamide-type alkaloid
Stenine-type alkaloid
Anti-TMV

ABSTRACT

Three new tuberostemoamide-type alkaloids, stemtuberolines A-C (1–3), four new stenine-type alkaloids, stemtuberolines D-G (4–7), together with five known *Stemona* alkaloids (8–12), were isolated from the roots of *Stemona tuberosa*. Their structures were elucidated on the basis of comprehensive spectroscopic data analysis. Stemtuberoline C (3) exhibited significant anti-TMV activity with an inhibition rate of 60.48% at the concentration of 50 µg/mL, while that of ningenmycin, the positive control, was 52.89%.

1. Introduction

Stemona alkaloids characterized by the presence of the pyrrolo[1,2-*a*]azepine nucleus were widely found in a large variety of Stemonaceae family [1,2]. As the largest genus of Stemonaceae, *Stemona* has been used as a source of insecticides and antitussive remedies for a long time in China, Japan, and Southeastern Asian countries [3]. In our previous study, several active substances against TMV had been isolated from the genus *Stemona* plants [4]. During a search for anti-TMV chemicals from natural sources [5–7], *S. tuberosa* was investigated and seven new *Stemona* alkaloids (1–7), including three tuberostemoamide-type and four stenine-type alkaloids were obtained. The structures of the new alkaloids were established on the basis of extensive spectroscopic analyses and their anti-TMV activities were also evaluated. Herein, the isolation, structure determination and bioactivities of the compounds are described.

2. Experimental

2.1. General

NMR spectra were measured via a Bruker AV-500 MHz, or a Bruker Avance III 600 MHz spectrometer, TMS was used as an internal

standard. ECD spectra were acquired with a Chirascan instrument. Optical rotations were recorded on a Horiba SEPA-300 polarimeter. ESIMS and HRESIMS were obtained on an API QSTAR Pulsar 1 spectrometer. Sephadex LH-20 (Amersham Pharmacia, Uppsala, Sweden), MCI gel CHP 20P (75–150 µm, Mitsubishi Chemical Industries, Tokyo, Japan), and RP-18 (20–45 µm; Daiso Co., Japan) were used for column chromatography. Silica gel (Qingdao Marine Chemical Inc., Qingdao, PR China) was used for preparative TLC. Semi-preparative HPLC was carried out using a Shimadzu SPD-20A liquid chromatograph equipped with a Phenomene Luna 5 µm C₁₈ (2) 100A column (250 mm × 10 mm, 5 µm).

2.2. Plant material

The roots of *S. tuberosa* were purchased from Kunming Luosiwan Chinese medicine market, in July 2017. The plant species was authenticated by Prof. Hua Peng, Kunming Institute of Botany, Chinese Academy of Science (CAS). The voucher specimen (KIB20170716) was deposited in the State Key Laboratory of Phytochemistry and Plant Resources in West China, Kunming Institute of Botany, CAS.

* Corresponding author at: State Key Laboratory of Functions and Applications of Medicinal Plants, Guizhou Medical University, Guiyang 550014, PR China.

** Corresponding author.

E-mail addresses: zhangyu@mail.kib.ac.cn (Y. Zhang), haoxj@mail.kib.ac.cn (X.-J. Hao).

¹ The first two authors contributed equally to this work.

2.3. Extraction and isolation

Dried and powdered *S. tuberosa* (40 kg) was extracted with MeOH under condition reflux to give a crude extract, which was suspended in 3% HCl followed by extraction with petroleum ether. The acidic aqueous extract was basified (pH 9–10) with 25% aqueous NH_4OH , and then extracted with CH_2Cl_2 , and evaporated the solvent under reduced pressure to afford a crude alkaloid extract (100 g). The crude alkaloid was further divided into four parts (Fr. A–D) by RP-18 column chromatography eluting with MeOH/ H_2O (10:90 to 100:0). Fr. A (17 g) was subsequently fractionated by a silica gel column eluting with CH_2Cl_2 /MeOH (200:1 to 40:1) gradient to provide four portions (Fr. A.1–A.4). Of these, Fr. A.1 (5 g) was subjected to Sephadex LH-20 (MeOH), followed by a silica gel (CH_2Cl_2 /MeOH, 50:1) to yield compounds **11** (2.3 g) and **12** (300 mg). Fr. A.2 (3 g) was subjected to Sephadex LH-20 (MeOH), followed by semi-preparative HPLC (MeOH- H_2O 25:75) to afford compounds **5** (5.4 mg, $t_R = 15$ min), **6** (6.5 mg, $t_R = 20$ min) and **7** (15.1 mg, $t_R = 22$ min). Fr. B (6.3 g) was subjected to Sephadex LH-20 (MeOH), followed by a silica gel (petroleum/acetone/ Et_2NH , 50:1:0.1 to 1:1:0.1) to yield compounds **8** (25 mg), **9** (13 mg), and **10** (9 mg). Fr. C (9 g) was subsequently fractionated by RP-18 column eluting with MeOH/ H_2O (40:60 to 100:0) gradient to provide three portions (Fr. C.1–C.3). Fr. C.2 (2.1 g) was purified by Sephadex LH-20 (MeOH), followed by semi-preparative HPLC (CH_3CN - H_2O , 35:65) to get compounds **1** (4.3 mg, $t_R = 13$ min), **2** (23 mg, $t_R = 23$ min), and **3** (8.7 mg, $t_R = 27$ min). Fr. C.3 (3.5 g) was purified by a silica gel (CH_2Cl_2 /MeOH, 100:1), followed by Sephadex LH-20 (MeOH) to yield compounds **4** (3.5 mg).

Stemtuberoline A (**1**): white solid; $[\alpha]_{20}^D - 25.1$ (c 0.17, MeOH); IR (KBr) ν_{max} 3439, 2936, 1733, 1437, 1196 cm^{-1} ; ^1H and ^{13}C NMR data (methanol- d_4 , 500 and 125 MHz), see Tables 1 and 2; HRESIMS m/z

Table 1

^1H NMR spectroscopic data for **1**, **2**, and **3** (δ in ppm, J in Hz).

Position	1 ^a	2 ^a	3 ^a
1a	1.78 m	1.94 m	2.16 m
1b	1.61 m	1.92 m	1.92 m
2a	1.93 m	1.90 m	2.15 m
2b	1.42 m	1.38 m	2.08 m
3	3.40 m	3.36 m	3.94 ddd (13.5, 8.0, 5.5)
5a	3.43 m	3.51 dd (15.5, 5.5)	3.85 dd (15.5, 5.5)
5b	2.91 m	2.98 dd (15.5, 12.0)	3.76 dd (15.5, 12.0)
6a	1.71 m	1.85 m	1.95 m
6b	1.20 m	1.38 m	1.93 m
7a	1.79 m	2.12 m	2.17 m
7b	1.41 m	1.41 m	1.63 m
8a	1.39 m	4.01 m	4.18 m
8b	1.15 m		
9	2.21 m	2.11 m	2.87 ddd (12.0, 9.5, 4.5)
9a	3.57 m	3.69 ddd (12.0, 8.5, 4.5)	4.25 ddd (12.0, 8.5, 4.5)
10	2.43 m	2.12 m	2.15 m
12a	2.85 m	2.52 d (13.5)	6.88 q (1.5)
12b	2.65 m	2.22 d (13.5)	
13	2.82 m		
15	1.15 d (7.0)	1.53 s	1.88 s
16a	1.63 m	1.74 m	1.46 m
16b	1.56 m	1.23 m	1.38 m
17	0.78 t (7.5)	0.97 t (7.5)	0.86 t (7.5)
18	4.22 ddd (11.0, 8.0, 5.5)	4.20 ddd (11.0, 8.0, 5.5)	5.10 ddd (11.0, 8.0, 5.5)
19a	2.42 m	2.42 m	2.48 ddd (12.0, 8.0, 5.5)
19b	1.58 m	1.60 m	1.76 m
20	2.69 m	2.69 m	2.78 m
22	1.20 d (7.0)	1.20 d (7.0)	1.22 d (7.0)
-OMe	3.63 s		

^a 500 MHz in methanol- d_4 .

Table 2

^{13}C NMR spectroscopic data for **1**, **2**, and **3** (δ in ppm).

Position	1 ^a	2 ^a	3 ^a
1	26.8 t	28.1 t	25.0 t
2	27.9 t	27.8 t	25.0 t
3	65.5 d	65.3 d	77.1 d
5	48.0 t	47.2 t	68.8 t
6	30.3 t	21.0 t	21.5 t
7	25.6 t	34.8 t	35.9 t
8	28.3 t	80.5 d	79.9 d
9	44.0 d	55.2 d	49.8 d
9a	63.7 d	61.7 d	87.3 d
10	57.8 d	53.2 d	51.8 d
11	214.2 s	115.6 s	114.3 s
12	47.8 t	44.7 t	146.6 d
13	35.7 d	74.6 s	134.7 s
14	178.0 s	180.2 s	173.1 s
15	17.3 q	25.5 q	10.4 q
16	23.5 t	26.0 t	20.5 t
17	11.2 q	11.8 q	12.8 q
18	84.9 d	85.2 d	75.4 d
19	35.6 t	35.6 t	35.6 t
20	36.1 d	36.0 d	35.9 d
21	182.1 s	182.1 s	180.7 s
22	15.0 q	15.0 q	14.7 q
OMe	52.3 q		

^a 125 MHz in methanol- d_4 .

z 408.2743 $[\text{M} + \text{H}]^+$ (calcd for $\text{C}_{23}\text{H}_{38}\text{NO}_5$, 408.2744).

Stemtuberoline B (**2**): white solid; $[\alpha]_{20}^D - 32.1$ (c 0.13, MeOH); IR (KBr) ν_{max} 3435, 2936, 1775, 1640, 1189 cm^{-1} ; ^1H and ^{13}C NMR data (methanol- d_4 , 500 and 125 MHz), see Tables 1 and 2; HRESIMS m/z 408.2383 $[\text{M} + \text{H}]^+$ (calcd for $\text{C}_{22}\text{H}_{34}\text{NO}_6$, 408.2381).

Stemtuberoline C (**3**): white solid; $[\alpha]_{20}^D - 115.3$ (c 0.1, MeOH); IR (KBr) ν_{max} 3431, 2935, 1769, 1458, 1161, 975 cm^{-1} ; ^1H and ^{13}C NMR data (methanol- d_4 , 500 and 125 MHz), see Tables 1 and 2; HRESIMS m/z 406.2224 $[\text{M} + \text{H}]^+$ (calcd for $\text{C}_{22}\text{H}_{32}\text{NO}_6$, 406.2224).

Stemtuberoline D (**4**): yellow solid; $[\alpha]_{20}^D - 78.3$ (c 0.2, MeOH); IR (KBr) ν_{max} 3435, 2970, 2879, 1767, 1456, 1170, 761 cm^{-1} ; ^1H and ^{13}C NMR data (DMSO- d_6 , 600 and 150 MHz), see Tables 3 and 4; HRESIMS m/z 394.2589 $[\text{M} + \text{H}]^+$ (calcd for $\text{C}_{22}\text{H}_{36}\text{NO}_5$, 394.2588).

Stemtuberoline E (**5**): white solid; $[\alpha]_{20}^D - 115.3$ (c 0.1, MeOH); IR (KBr) ν_{max} 3435, 2937, 1767, 1456, 1170, 997 cm^{-1} ; ^1H and ^{13}C NMR data (DMSO- d_6 , 500 and 125 MHz), see Tables 3 and 4; HRESIMS m/z 394.1986 $[\text{M} + \text{H}]^+$ (calcd for $\text{C}_{22}\text{H}_{30}\text{NO}_4$, 394.1989).

Stemtuberoline F (**6**): white solid; $[\alpha]_{20}^D + 25.2$ (c 0.11, MeOH); IR (KBr) ν_{max} 3431, 2936, 1767, 1458, 1168, 926 cm^{-1} ; ^1H and ^{13}C NMR data (acetone- d_6 , 500 and 125 MHz), see Tables 3 and 4; HRESIMS m/z 392.2432 $[\text{M} + \text{H}]^+$ (calcd for $\text{C}_{22}\text{H}_{34}\text{NO}_5$, 392.2431).

Stemtuberoline G (**7**): white solid; $[\alpha]_{20}^D + 36.5$ (c 0.18, MeOH); IR (KBr) ν_{max} 3431, 2936, 1770, 1458, 1198, 1167, 926 cm^{-1} ; ^1H and ^{13}C NMR data (acetone- d_6 , 500 and 125 MHz), see Tables 3 and 4; HRESIMS m/z 392.2434 $[\text{M} + \text{H}]^+$ (calcd for $\text{C}_{22}\text{H}_{34}\text{NO}_5$, 392.2431).

2.4. Anti-TMV activities

Protective effect in vivo: The compound solutions (50 $\mu\text{g}/\text{mL}$) were smeared on the left side of the leaves of *N. glutinosa*, whereas the right side of the leaves was inoculated with the DMSO solution as a negative control. After 6 h, 100 μL of TMV particles (50 $\mu\text{g}/\text{mL}$) were inoculated onto the whole leaf, and then the inoculated leaf was washed with water after 10 min. The local lesion numbers were recorded 3 days after inoculation [8,9].

Curative effect in vivo: TMV particles (50 $\mu\text{g}/\text{mL}$) were inoculated onto whole leaves of *N. glutinosa*. After 24 h, the compound solutions (50 $\mu\text{g}/\text{mL}$) were smeared onto the left half of TMV-inoculated leaf, while the DMSO solution was smeared onto the right side as a negative control. The local lesion numbers were recorded 3 days after

Table 3
¹H NMR spectroscopic data for **4**, **5**, **6**, and **7** (δ in ppm, J in Hz).

Position	4 ^a	5 ^b	6 ^c	7 ^c
1	1.58 m		2.14 m	2.23 m
2a	1.61 m	6.0 s	2.49 m	2.54 m
2b	1.50 m		1.83 m	1.89 m
3	3.05 m		3.80 m	3.97 m
5a	2.98 m	4.16 m	3.69 dd (13.0, 6.0)	3.83 dd (13.0, 6.0)
5b	2.85 m	3.62 m	3.45 t (11.5)	3.56 t (11.5)
6a	1.65 m	1.91 m	2.76 m	2.66 m
6b	1.44 m	1.46 m	1.58 m	1.69 m
7a	1.54 m	1.93 m	2.06 m	2.12 m
7b	1.36 m	1.58 m	1.95 m	1.97 m
8a	1.87 m	2.07 m	1.66 m	1.69 m
8b	1.48 m	1.04 m	1.58 m	1.61 m
9	1.61 m	2.29 m	2.02 m	2.08 m
9a	3.26 dd (7.0, 5.0)		4.32 dd (7.0, 5.0)	4.39 dd (7.0, 5.0)
10	1.70 m	1.29 m	2.12 m	2.15 m
11	4.57 t (3.0)	4.75 m	4.74 t (3.0)	4.75 t (3.0)
12	2.00 m	3.38 m	2.60 m	2.66 m
13	3.01 m	3.10 m	3.07 m	3.08 m
15	1.08 d (7.0)	1.13 d (7.0)	1.21 d (7.0)	1.20 d (7.0)
16a	1.61 m	1.75 m	1.74 m	1.75 m
16b	1.14 m	1.53 m	1.23 m	1.24 m
17	0.94 t (7.5)	1.00 t (7.5)	1.01 t (7.5)	1.01 t (7.5)
18	3.52 ddd (11.5, 7.5, 5.5)	5.69 t (7.0)	5.44 ddd (11.5, 7.5, 5.5)	5.36 ddd (11.5, 7.5, 5.5)
19a	1.58 m	2.63 m	2.47 m	2.51 m
19b	1.32 m	2.13 m	1.79 m	1.83 m
20	2.46 m	2.76 m	2.72 m	2.73 m
22	1.01 d (7.0)	1.20 d (7.0)	1.15 d (7.0)	1.15 d (7.0)

^a 600 MHz in DMSO-*d*₆; ^b 500 MHz in DMSO-*d*₆; ^c 500 MHz in acetone-*d*₆.**Table 4**
¹³C NMR spectroscopic data for **4**, **5**, **6**, and **7** (δ in ppm).

Position	4 ^a	5 ^b	6 ^c	7 ^c
1	36.2 d	109.7 s	34.4 d	34.5 d
2	32.6 t	106.3 d	31.2 t	31.4 t
3	67.8 d	135.0 s	81.4 d	81.9 d
5	51.1 t	45.6 t	67.2 t	67.2 t
6	30.2 t	28.5 t	23.2 t	23.5 t
7	22.8 t	29.1 t	28.2 t	28.2 t
8	29.4 t	33.5 t	23.6 t	23.5 t
9	34.4 d	35.2 d	35.5 d	35.5 d
9a	66.0 d	129.1 s	94.3 d	93.8 d
10	36.9 d	43.6 d	35.6 d	35.6 d
11	78.0 d	77.4 d	77.8 d	77.7 d
12	40.3 d	38.5 d	39.9 d	39.8 d
13	41.8 d	41.3 d	43.1 d	43.1 d
14	178.8 s	178.5 s	178.5 s	178.5 s
15	10.0 q	11.5 q	10.2 q	10.1 q
16	20.8 t	22.9 t	21.5 t	21.1 t
17	10.9 q	11.9 q	10.9 q	10.9 q
18	69.3 d	71.4 d	75.2 d	75.0 d
19	36.3 t	33.6 t	35.2 t	35.2 t
20	35.5 d	34.6 d	35.2 d	35.2 d
21	178.3 s	179.4 s	178.9 s	178.8 s
22	16.2 q	15.5 q	14.8 q	14.8 q

^a 150 MHz in DMSO-*d*₆; ^b 125 MHz in DMSO-*d*₆; ^c 125 MHz in acetone-*d*₆.

inoculation [8,9].

3. Results and discussion

Stemtuberoline A (**1**) was obtained as a white solid, and its molecular formula was assigned as C₂₃H₃₇NO₅, from its HRESIMS (m/z 408.2743 [M + H]⁺, calcd for 408.2744) and NMR data (Tables 1 and 2). The IR spectrum clearly exhibited absorption band of ester carbonyl

(1733 cm⁻¹) functionality. The ¹H NMR data (Table 1) showed the signals of three methyls (δ_{H} 1.20, d, J = 7.0 Hz; δ_{H} 1.15 d, J = 7.0 Hz; δ_{H} 0.78 t, J = 7.5 Hz) and one methoxy group (δ_{H} 3.63, s). The ¹³C and DEPT NMR data displayed resonances including four methyls, nine methylenes, seven methines, and three quaternary carbons (Table 2). The aforementioned evidences suggested that compound **1** was an analogue of tuberostemoamide-type alkaloid [10]. ¹H – ¹H COSY correlations of H₂-5/H₂-6/H₂-7/H₂-8/H-9/H-10/H₂-16/H₃-17 and H-9a/H₂-1/H₂-2/H-3/H-18/H₂-19/H-20/H₃-22, together with the HMBC correlations of H-3 (δ_{H} 3.40) to C-5 (δ_{C} 48.0), and of H₂-19 (δ_{H} 2.42, 1.58) and H₃-22 (δ_{H} 1.20, d, J = 7.0 Hz) to C-21 (δ_{C} 182.1) indicated the existence of a pyrrolo[1,2- α]azepine core with an α -methyl- γ -lactone moiety substituent at C-3 (Fig. 1). Meanwhile, ¹H – ¹H COSY correlations of H₂-12/H-13/H₃-15 and HMBC correlations of H-13 (δ_{H} 2.82) to C-11 (δ_{C} 214.2), and of H₃-15 (δ_{H} 1.15, d, J = 7.0 Hz) and H₂-12 (δ_{H} 2.85, 2.65) to C-14 (δ_{C} 178.0) indicated the existence of a methyl 2-methyl-4-oxobutanoate moiety. HMBC cross-peaks of H₂-16 (δ_{H} 1.63, 1.56) and H-9 (δ_{H} 2.21) to C-11 led to the connections of the methyl 2-methyl-4-oxobutanoate moiety to pyrrolo[1,2- α]azepine core via C-10. Thus, the planar structure of **1** was established as depicted.

The relative configuration of **1** was deduced from the analysis of its ROESY spectrum in combination with its biogenetic consideration (Fig. 3). The ROESY correlations of H₃-21/H₂-19b, H₂-19b/H-3, and H-3/H₂-5a indicated that both protons were cofacial and were arbitrarily assigned as α -oriented. Accordingly, the correlations of H₂-5b/H-9, H-9/H₂-16a, H-18/H-20, H₂-19a/H₂-2a, and H₂-2a/H-9a suggested that H-18, H-9 and H-9a were all β -oriented. However, the stereochemistry of C-10 and C-13 remained unknown due to the free rotation of the single C–C bond. Therefore, the relative configuration of **1** was assigned as 3S*, 9R*, 9aS*, 18S*, and 20S*.

Stemtuberoline B (**2**) was obtained as a white solid, and was assigned the molecular formula C₂₂H₃₃NO₆ based on HRESIMS m/z 408.2383 [M + H]⁺ (calcd for 408.2381). The IR absorptions at 1775 and 3435 cm⁻¹ indicated the existence of an ester carbonyl and a hydroxyl group, respectively. The ¹H and ¹³C NMR data (Tables 1 and 2) of compound **2** suggested that **2** were very similar to those of dihydrostemoninine [11], except for signals arising from a geminal coupling CH₂ group (δ_{H} 2.52, d, J = 13.5 Hz, H-12a; δ_{H} 2.22, d, J = 13.5 Hz, H-12b) and an additional quaternary carbon (δ_{C} 74.6C-13). This information, in combination with HRESIMS, indicated that **2** was a hydroxyl derivative of dihydrostemoninine. In addition, HMBC correlations of H-12 and H₃-15 (δ_{H} 1.53 s) to C-13 demonstrated that the hydroxyl group was located at C-13 (Fig. 2). The relative configuration of **2** was similar to that of dihydrostemoninine. Meanwhile, the correlations of H₂-16b/H₂-12a, and H₂-12b/H₃-15 indicated that H₃-15 was α -oriented (Fig. 3). Accordingly, the relative configuration of **2** was established as 3S*, 8R*, 9R*, 9aS*, 10S*, 11S*, 13S*, 18S* and 20S*.

Stemtuberoline C (**3**) was obtained as a white solid, and was assigned the molecular formula of C₂₂H₃₁NO₆ based on HRESIMS m/z 406.2224 [M + H]⁺ (calcd for 406.2224). The ¹H and ¹³C NMR data (Tables 1 and 2) suggested that compound **3** had a great similarity with that of stemoninine (**8**) [12]. The most notable differences were the signals at C-3, C-5, and C-9a in stemoninine were downfield shifted $\Delta\delta$ + 13.7, +20.3, and + 21.5 ppm in **3**, respectively. Furthermore, the molecular weight of **3** is 16 mass units larger than that of **8**, indicated that compound **3** was the *N*-oxide form of **8**. The relative configuration of **3** was shown to be identical to that of **8** based on their similar coupling constants and supported by the ROESY data. The up-field shift of the C-9 ($\Delta\delta$ = -4.1 ppm) compared with that of **8** revealed that oxygen atom at N-4 adopted β configuration as same as H-9 due to the γ -gauche effect [13–15].

Stemtuberoline D (**4**) was obtained as a yellow solid, and its molecular formula, C₂₂H₃₅NO₅, was established via HRESIMS m/z 394.2589 [M + H]⁺ (calcd for 394.2588). Detailed analysis of the NMR data of **4** (Tables 3 and 4) indicated that **4** shared the same basic skeleton with that of neutuberostemoninine (**11**) [16]. The striking differences were the

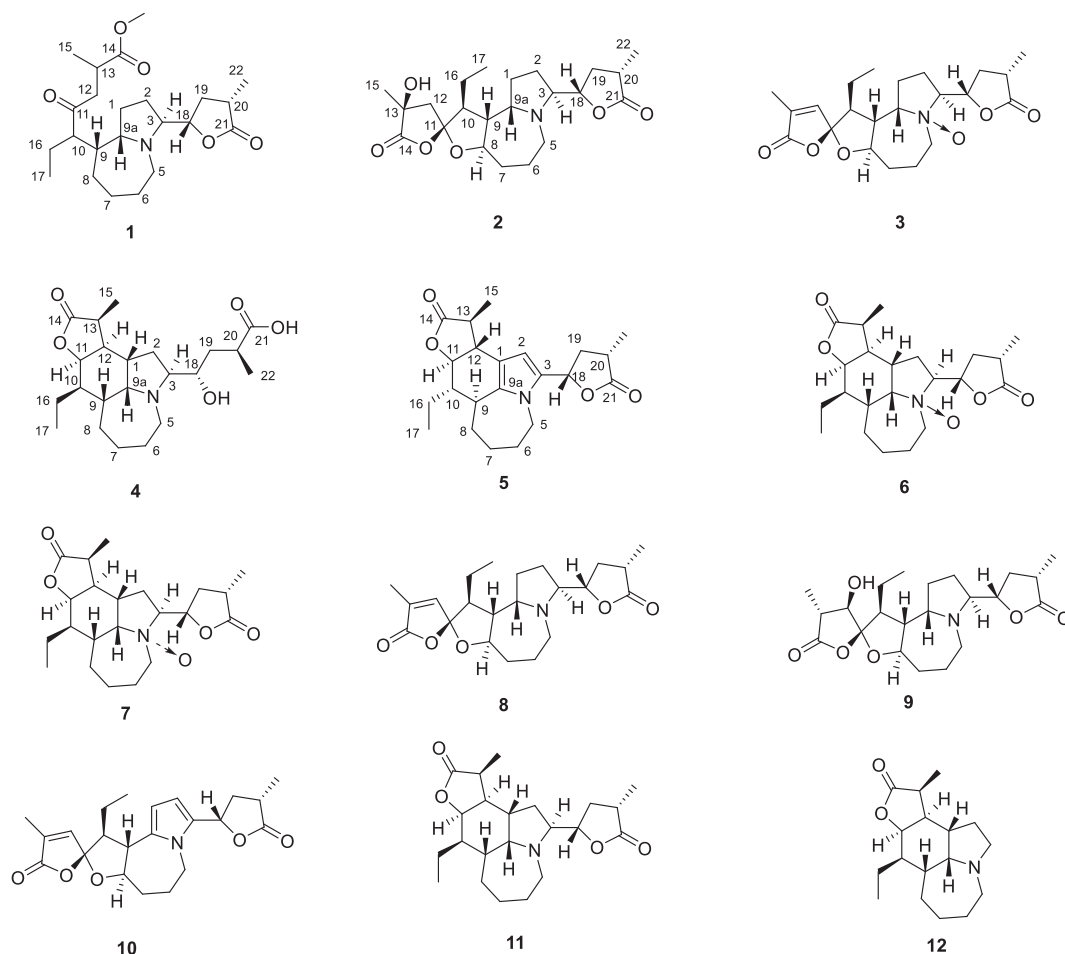


Fig. 1. Chemical structures of compounds 1–12.

molecular weight of **4** was 18 mass units more than that of **11** and the index of hydrogen deficiency of **4** was one less than that of **11**. Thus **4** was assumed to be a cleavage product of **11**, and the disappeared HMBC correlation of H-18 to C-21 indicated that the hydrolyzation took place in the α -methyl- γ -lactone moiety.

Stemtuberoline E (**5**) was isolated as a white solid, and have a molecular formula of $C_{22}H_{29}NO_4$ based on HRESIMS m/z 394.1986 $[M + H]^+$ (calcd for 394.1989). Comparison of the NMR data of **5** (Tables 3 and 4) with those of 9α -bisdehydrotuberostemonine [17], showed that both alkaloids shared the same planar structure. The observation of the downfield shifts of H-11 (δ_H 4.75, $\Delta\delta_H + 0.35$) and H-

12 (δ_H 3.38, $\Delta\delta_H + 0.21$), as well as upfield shifts of C-9 (δ_C 35.2, $\Delta\delta_C - 1.1$), C-11 (δ_C 77.4, $\Delta\delta_C - 2.2$), and C-12 (δ_C 38.5, $\Delta\delta_C - 2.7$) in **5** indicated that **5** might be an epimer of 9α -bisdehydrotuberostemonine at the positions of C-10 and C-11 due to their steric effect. Furthermore, the key ROESY correlations of H-10/H-12, H-9/H-11, and H-11/H-13 (Fig. 3) confirmed the above elucidation.

Stemtuberoline F (**6**) was obtained as a white solid, and was assigned the molecular formula $C_{22}H_{33}NO_5$ based on HRESIMS m/z 392.2432 $[M + H]^+$ (calcd for 392.2431). Comparison of the NMR data of **6** (Tables 3 and 4) to those of neutuberostemonine (**11**) [16] showed that they were closely related analogues featuring identical

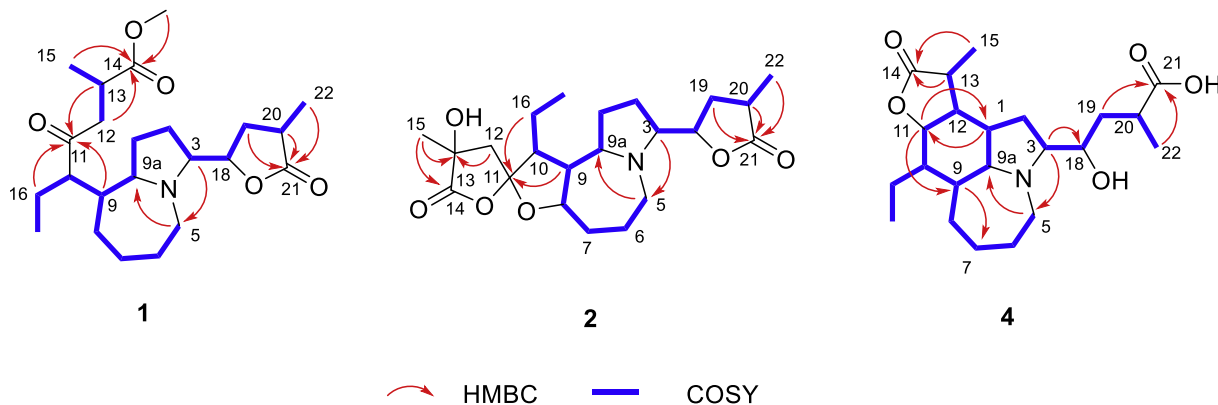


Fig. 2. Key HMBC and 1H - 1H COSY correlations of compounds 1, 2, and 4.

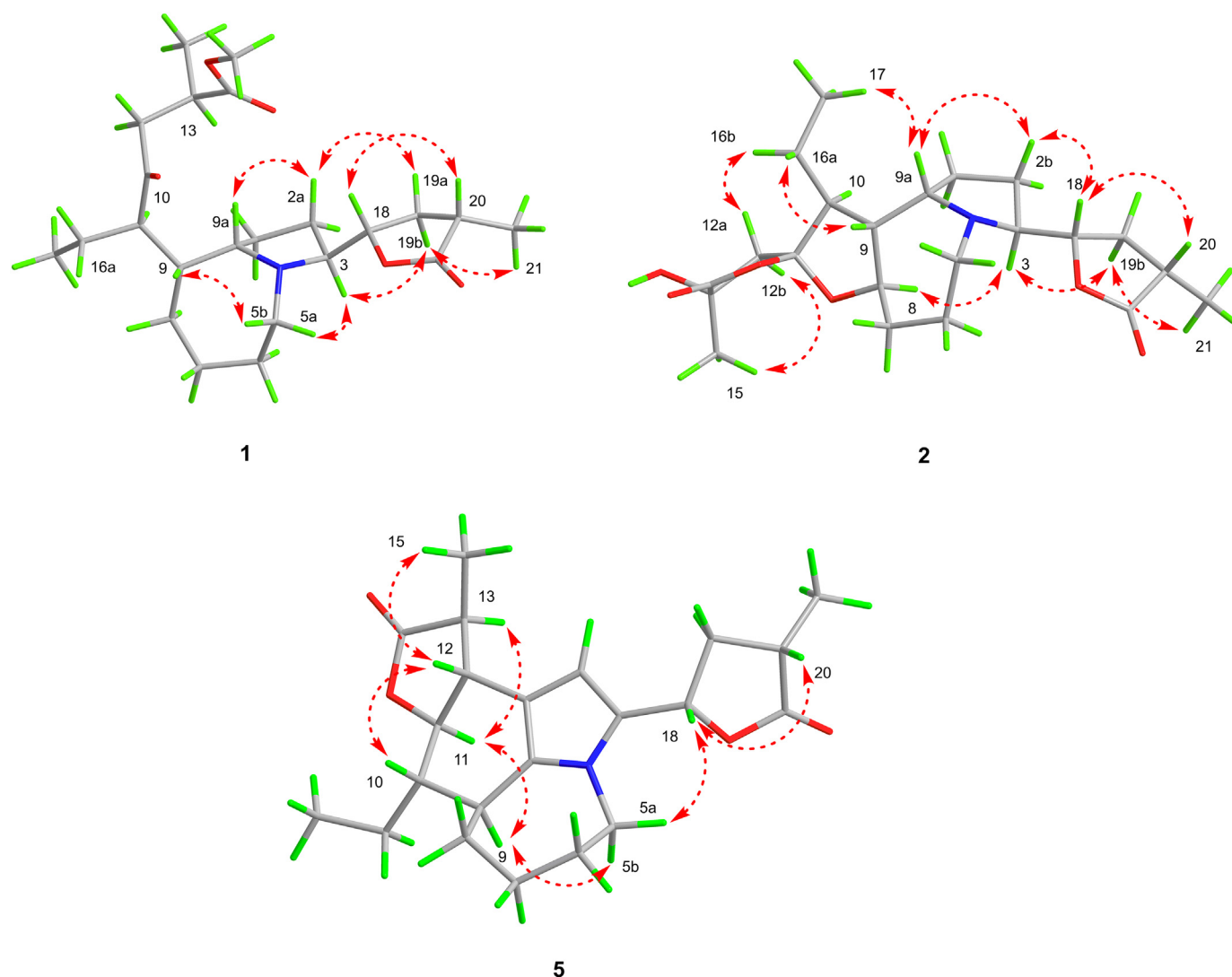


Fig. 3. Key ROESY correlations of compounds 1, 2, and 5.

carbon frameworks. The main distinction was that the carbon signals of C-3, C-5 and C-9a in **6** were shifted downfield by 13.8, 16.4, and 17.1 ppm, respectively. All these data suggested that these three carbons should be attached to the *N*-oxide group, which was further confirmed by 2D-NMR experiments. The relative configurations of all the chiral carbons of **6** were consistent with those of **11** as determined by similar ROESY correlations. Moreover, by comparison of the NMR data of **6** with that of **11**, the resonance of the C-18 is 6.3 ppm to low frequency ($\Delta\delta = -6.3$ ppm), which indicated that the oxygen atom at N-4 adopted β configuration as same as H-18 due to the obvious γ -gauche effect [15].

Stemtuberoline G (**7**) was isolated as a white solid, and was assigned to have a molecular formula of $C_{22}H_{33}NO_5$ based on HRESIMS m/z 392.2434 $[M + H]^+$ (calcd for 392.2431). Detailed analysis of the NMR data (Tables 3 and 4) indicated **7** shared the same planar structure with that of **6**. The relative configurations of all the chiral carbons of **7** were shown to be identical to that of **6** based on their similar coupling constants and supported by the ROESY data. Moreover, the observation of the downfield shifts of H-3 ($\Delta\delta + 0.17$ ppm), H-5a ($\Delta\delta + 0.14$ ppm) and H-5b ($\Delta\delta + 0.11$ ppm) in **7** revealed that oxygen atom at N-4 adopted α configuration.

Five known compounds (**8**–**12**) were respectively identified as stemoninine (**8**) [12], oxystemoninine (**9**) [18], isobisdehydrostemoninine (**10**) [19], neotuberostemoninine (**11**) [16] and neostenine (**12**) [20], by

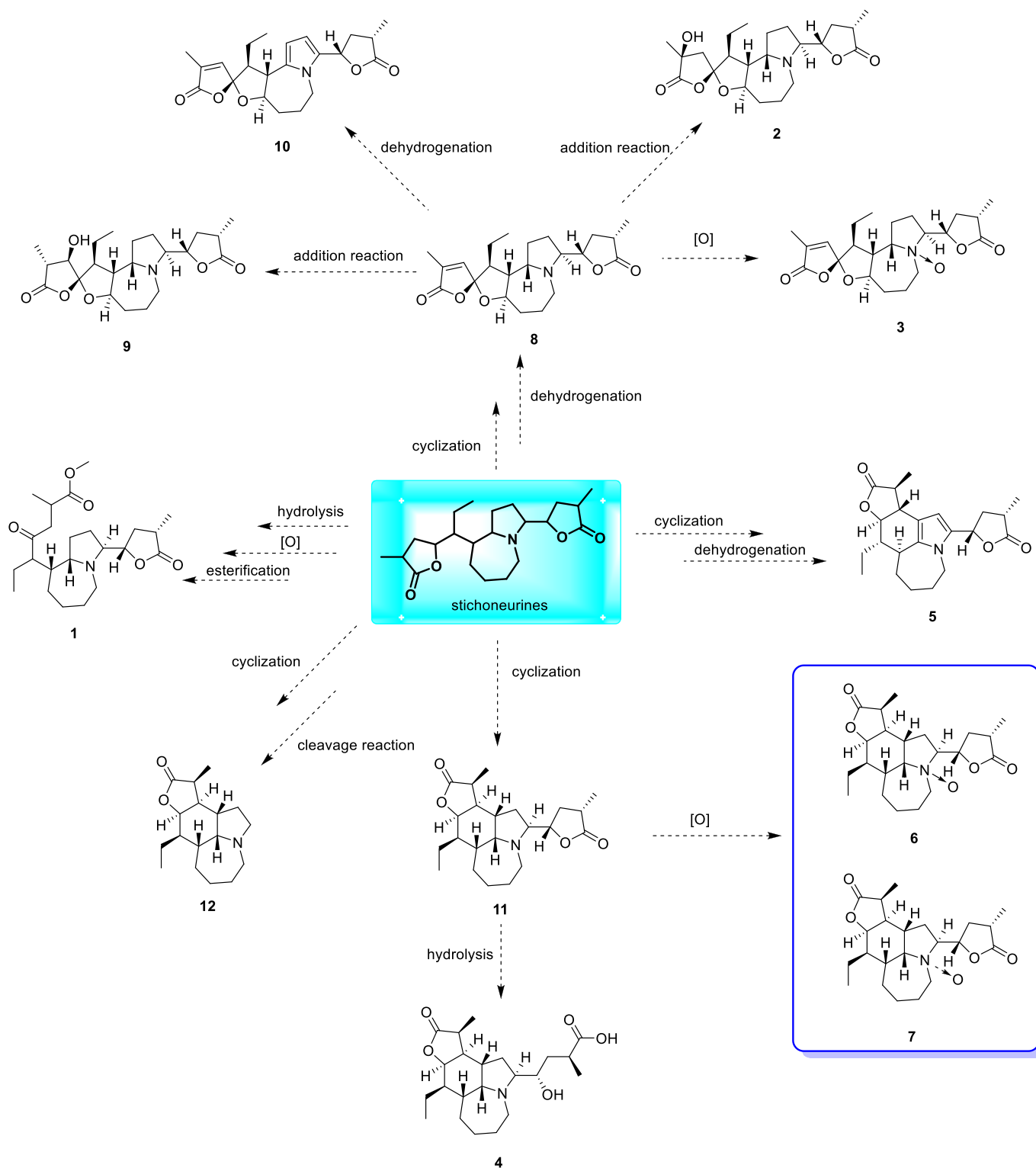
comparison of their spectroscopic data with those literatures.

A plausible biogenetic relationship between compounds **1**–**12** was proposed in Scheme 1. The biogenetic precursor of **1**–**12** seems to be stichoneurines [21–24], which undergo complex sequence of steps involving cyclization, dehydrogenation and cleavage reaction to obtain compounds **5**, **8**, **11** and **12**. Compound **1** might be originated from stichoneurine A through hydrolysis, oxidation and esterification sequence [24]. Compound **8** underwent dehydrogenation, addition reaction and oxidation to obtain compounds **10**, **2**, **9** and **3**, respectively. Compound **11** underwent hydrolysis and oxidation to obtain compounds **4**, **6** and **7**, respectively.

The anti-TMV activity of 12 *Stemona* alkaloids was tested in *Nicotiana glutinosa* using the half-leaf method for the first time. The results showed that compound **3** exhibited the best activity at concentration of 50 $\mu\text{g/mL}$, with the curative inhibition rate of 60.48%, which was higher than that of ningnamycin (52.89%). However, compound **3** exhibited no protective efficacy against TMV.

Declaration of Competing Interest

We declare no conflict of interest for this study.



Scheme 1. Proposed biosynthetic pathways of 1–12.

Acknowledgments

This research was supported financially by grants from the National Science Foundation of China (U1812403), Top Young Talent of the Ten Thousand Talents Program of Yunnan (to Y.Z.), the Young Academic and Technical Leader Raising Foundation of Yunnan (to Y.Z.), the Science and Technology Department of Guizhou Province (QKH JC-[2020]-1Y398), the Special Project of Academic Young Cultivation and

Innovation Exploration of Guizhou Medical University (QKH PTRC [2018] 5779-60), and Guizhou Provincial Engineering Research Center for Natural Drugs.

Appendix A. Supplementary data

Supplementary data to this article can be found online at <https://doi.org/10.1016/j.fitote.2020.104572>

References

- [1] R.W. Jiang, P.M. Hon, Y.T. Xu, Y.M. Chan, H.X. Xu, P.C. Shaw, P.P. But, Isolation and chemotaxonomic significance of tuberostemospironine-type alkaloids from *Stemona tuberosa*, *Phytochemistry* 67 (2006) 52–57.
- [2] S. Kongkiatpaiboon, J. Schinnerl, S. Felsing, V. Keeratinijakal, S. Vajrodaya, W. Gritsanapan, L. Brecker, H. Greger, Structural relationships of *Stemona* alkaloids: assessment of species-specific accumulation trends for exploiting their biological activities, *J. Nat. Prod.* 74 (2011) 1931–1938.
- [3] Y. Wu, L.T. Ou, D. Han, Y.B. Tong, M. Zhang, X.H. Xu, C.F. Zhang, Pharmacokinetics, biodistribution and excretion studies of neotuberostemone, a major bioactive alkaloid of *Stemona tuberosa*, *Fitoterapia* 112 (2016) 22–29.
- [4] Z.X. Hu, H.Y. Tang, J. Guo, H.A. Aisa, Y. Zhang, X.J. Hao, Alkaloids from the roots of *Stemona tuberosa* and their anti-tobacco mosaic virus activities, *Tetrahedron* 75 (2019) 1711–1716.
- [5] J. Chen, X.H. Yan, J.H. Dong, P. Sang, X. Fang, Y.T. Di, Z.K. Zhang, X.J. Hao, Tobacco mosaic virus (TMV) inhibitors from *Picrasma quassioides* Benn, *J. Agric. Food Chem.* 57 (2009) 6590–6595.
- [6] L.J. Huang, Y.H. Ge, K.X. Liu, J.X. Zhang, X.J. Hao, Chemical constituents from *Aconitum recemulosum* effect against TMV, *Agrochemicals* 52 (2013) 295–297.
- [7] J.Y. Jian, K.X. Liu, Z.L. Di, Y.H. Ge, X.J. Hao, Alkaloids of *Aconitum carmichaeli* Debx and against TMV activity, *Agrochemicals* 10 (2017) 767–770.
- [8] L. Zhao, J. Dong, Z. Hu, S. Li, X. Su, J. Zhang, Y. Yin, T. Xu, Z. Zhang, H. Chen, Anti-TMV activity and functional mechanisms of two sesquiterpenoids isolated from *Tithonia diversifolia*, *Pestic. Biochem. Physiol.* 140 (2017) 24–29.
- [9] Q.F. Hu, B. Zhou, X.M. Gao, L.Y. Yang, L.D. Shu, Y.Q. Shen, G.P. Li, C.T. Che, G.Y. Yang, Antiviral chromones from the stem of *Cassia siamea*, *J. Nat. Prod.* 75 (2012) 1909–1914.
- [10] F.P. Wang, Q.H. Chen, *Stemona* alkaloids: biosynthesis, classification, and biogenetic relationships, *Nat. Prod. Commun.* 9 (2014) 1671–1824.
- [11] P. Wang, A.L. Liu, Z. An, Z.H. Li, G.H. Du, H.L. Qin, Novel alkaloids from the roots of *Stemona sessilifolia*, *Chem. Biodivers.* 4 (2007) 523–530.
- [12] D.L. Cheng, J. Guo, T.T. Chu, E. Röder, A study of *Stemona* alkaloids, III. Application of 2D-NMR spectroscopy in the structure determination of stemonine, *J. Nat. Prod.* 51 (1988) 202–211.
- [13] M. Barfield, S.H. Yamamura, Ab initio IGLO studies of the conformational dependencies of α -, β -, and γ -substituent effects in the ^{13}C NMR spectra of aliphatic and alicyclic hydrocarbons, *J. Am. Chem. Soc.* 112 (1990) 4747–4758.
- [14] W. Zhang, Y.W. GUO, K. Krohn, Macropodumines A–C: novel pentacyclic alkaloids with an unusual skeleton or zwitterion moiety from *Daphniphyllum macropodum* Miq, *Chem. Eur. J.* 12 (2006) 5122–5127.
- [15] J.H. Zhang, J.J. Guo, Y.X. Yuan, Y.H. Fu, Y.C. Gu, Y. Zhang, D.Z. Chen, S.L. Li, Y.T. Di, X.J. Hao, Four new tetracyclic alkaloids with *cis*-decahydroquinoline motif from *Myrioneuron effusum*, *Fitoterapia* 112 (2016) 217–221.
- [16] H.S. Chung, P.M. Hon, G. Lin, P.P. But, H. Dong, Antitussive activity of *Stemona* alkaloids from *Stemona tuberosa*, *Planta Med.* 69 (2003) 914–920.
- [17] L.G. Lin, H.P. Leung, J.Y. Zhu, C.P. Tang, C.Q. Ke, J.A. Rudd, G. Lin, Y. Ye, Croomine- and tuberostemone-type alkaloids from roots of *Stemona tuberosa* and their antitussive activity, *Tetrahedron* 64 (2008) 10155–10161.
- [18] L.G. Lin, K.M. Li, C.P. Tang, C.Q. Ke, J.A. Rudd, G. Lin, Y. Ye, Antitussive Stemonine alkaloids from the roots of *Stemona tuberosa*, *J. Nat. Prod.* 71 (2008) 1107–1110.
- [19] L.G. Lin, Q.X. Zhong, T.Y. Cheng, C.P. Tang, C.Q. Ke, G. Lin, Y. Ye, Stemonines from the roots of *Stemona tuberosa*, *J. Nat. Prod.* 69 (2006) 1051–1054.
- [20] R.W. Jiang, W.C. Ye, P.C. Shaw, P.P. But, T.C.W. Mak, Absolute configuration of neostenine, *J. Mol. Struct.* 966 (2010) 18–22.
- [21] S. Kongkiatpaiboon, J. Schinnerl, S. Felsing, V. Keeratinijakal, S. Vajrodaya, W. Gritsanapan, L. Brecker, H. Greger, Structural relationships of *Stemona* alkaloids: assessment of species-specific accumulation trends for exploiting their biological activities, *J. Nat. Prod.* 74 (2011) 1931–1938.
- [22] H. Greger, Structural relationships, distribution and biological activities of *Stemona* alkaloids, *Planta Med.* 72 (2006) 99–113.
- [23] R.A. Pilli, M.C. Ferreira de Oliveira, Recent progress in the chemistry of the *Stemona* alkaloids, *Nat. Prod. Rep.* 17 (2000) 117–127.
- [24] F.P. Wang, Q.H. Chen, *Stemona* alkaloids: biosynthesis, classification, and biogenetic relationships, *Nat. Prod. Commun.* 9 (2014) 1809–1822.